Two-dimensional photonic crystals with large complete photonic band gaps in both TE and TM polarizations

Feng Wen, Sylvain David*, Xavier Checoury, Moustafa El Kurdi, Philippe Boucaud

Institut d'Electronique Fondamentale, Bât. 220 CNRS - Univ Paris Sud 91405 Orsay, France
* Corresponding author: sylvain.david@ief.u-psud.fr

http://www.u-psud.fr/ief

Abstract: Photonic crystals exhibiting a photonic band gap in both TE and TM polarizations are particularly interesting for a better control of light confinement. The simultaneous achievement of large band gaps in both polarizations requires to reduce the symmetry properties of the photonic crystal lattice. In this letter, we propose two different designs of two-dimensional photonic crystals patterned in high refractive index thin silicon slabs. These slabs are known to limit the opening of photonic band gaps for both polarizations. The proposed designs exhibit large complete photonic band gaps : the first photonic crystal structure is based on the honey-comb lattice with two different hole radii and the second structure is based on a "tri-ellipse" pattern in a triangular lattice. Photonic band gap calculations show that these structures offer large complete photonic band gaps $\frac{\Delta\omega}{\omega}$ larger than 10 % between first and second photonic bands. This figure of merit is obtained with single-mode slab waveguides and is not restricted to modes below light cone.

© 2008 Optical Society of America

OCIS codes: (230.0230) optical devices ; (230.5298) photonic crystals.

References

1. Y. Akahane, T. Asano, B. S. Song, and S. Noda, "High-Q photonic nanocavity in a two-dimensional photonic crystal," Nature **425**, 944–947 (2003).
2. S. Noda, M. Fujita, and T. Asano, "Spontaneous-emission control by photonic crystals and nanocavities," Nature Photonics **1**, 449–458 (2007).
3. E. Weidner, S. Combrie, N. V. Q. Tran, A. De Rossi, J. Nagle, S. Cassette, A. Talneau, and H. Benisty, "Achievement of ultrahigh quality factors in GaAs photonic crystal membrane nanocavity," Appl. Phys. Lett. **89**, 221104 (2006).
4. T. Tanabe, M. Notomi, E. Kuramochi, and H. Taniyama, "Large pulse delay and small group velocity achieved using ultrahigh-Q photonic crystal nanocavities," Opt. Express **15**, 7826–7839 (2007).
5. S. G. Johnson, S. H. Fan, P. R. Villeneuve, J. D. Joannopoulos, and L. A. Kolodziejski, "Guided modes in photonic crystal slabs," Phys. Rev. B **60**, 5751–5758 (1999).
6. Y. Tanaka, T. Asano, Y. Akahane, B. S. Song, and S. Noda, "Theoretical investigation of a two-dimensional photonic crystal slab with truncated cone air holes," Appl. Phys. Lett. **82**, 1661–1663 (2003).
7. N. Li, M. Arita, S. Kako, M. Kitamura, S. Iwamoto, and Y. Arakawa, "Fabrication and optical characterization of III-nitride air-bridge photonic crystal with GaN quantum dots," Phys. Status Solidi C - Current Topics In Solid State Physics, **4**, 90–94 (2007).
8. Z. Zhang, T. Yoshie, X. Zhu, J. Xu, and A. Scherer, "Visible two-dimensional photonic crystal slab laser," Appl. Phys. Lett. **89**, 071102 (2006).

---

9. S. David, M. El kurdi, P. Boucaud, A. Chelnokov, V. Le Thanh, D. Bouchier, and J. M. Lourtioz, "Two-dimensional photonic crystals with Ge/Si self-assembled islands," Appl. Phys. Lett. **83**, 2509–2511 (2003).
10. X. Li, P. Boucaud, X. Checoury, O. Kermarrec, Y. Campidelli, and D. Bensahel, "Probing photonic crystals on silicon-on-insulator with Ge/Si self-assembled islands as an internal source," J. Appl. Phys. **99**, 023103 (2006).
11. D. Cassagne, C. Jouanin, and D. Bertho, "Hexagonal photonic-band-gap structures," Phys. Rev. B **53**, 7134–7142 (1996).
12. R. Z. Wang, X. H. Wang, B. Y. Gu, and G. Z. Yang, "Effects of shapes and orientations of scatterers and lattice symmetries on the photonic band gap in two-dimensional photonic crystals," J. Appl. Phys. **90**, 4307–4313 (2001).
13. W. M. Kuang, Z. L. Hou, Y. Y. Liu, and H. Li, "The bandgap of a photonic crystal with triangular dielectric rods in a honeycomb lattice," J. Opt. A-Pure Appl. Opt. **7**, 525–528 (2005).
14. C. G. Bostan and R. M. de Ridder, "Design of photonic crystal slab structures with absolute gaps in guided modes," J. Optoelectron. Adv. Mat. **4**, 921–928 (2002).
15. S. Takayama, H. Kitagawa, Y. Tanaka, T. Asano, and S. Noda, "Experimental demonstration of complete photonic band gap in two-dimensional photonic crystal slabs," Appl. Phys. Lett. **87**, 061107 (2005).
16. K. Sakoda, *Optical Properties of Photonic Crystals* (Springer, 2005).
17. L. C. Andreani and D. Gerace, "Photonic-crystal slabs with a triangular lattice of triangular holes investigated using a guided-mode expansion method," Phys. Rev. B **73**, 235114 (2006).

1. Introduction

Photonic crystals are being intensively studied for their ability to confine light in small mode volumes of the order of $(\lambda/n)^3$ and in optical modes with very high quality factors [1]. Traditionally, two-dimensional photonic crystals are periodic structures constituted of holes etched in dielectric slabs with square, hexagonal or honey-comb lattices. These lattices combining simplicity and quasi-isotropy of their Brillouin zone allow to open photonic band gaps. Such structures are usually used with point or linear defects to spatially confine light in the plane by photonic band gap and off-plane because of refractive index contrast.

It is well known that standard photonic crystals exhibit a forbidden band in only one polarization. The best quality factors of photonic crystal cavities have been measured with membrane configuration [2, 3, 4]. In this case, due to the vertical symmetry, TE-like and TM-like polarizations are not coupled [5] and thus do not decrease the quality factor of the optical resonances. However, the membrane approach is not optimal for the integration of photonic crystals on chips because of thermal management problems and mechanical stability. To address this issue, an alternative approach for silicon-based photonic crystals is to use silicon-on-insulator substrates or emitter materials reported on silicon and silicon oxide. In the latter case, the vertical confinements by the refractive index are often asymmetric. This asymmetry induces some coupling between TE-like and TM-like polarizations and reduces the quality factor of confined modes. Alternately, the limitations of etching processes [6] which do not allow to obtain vertical pattern walls as shown in GaN [7] or GaP [8] devices induce also a coupling between TE-like and TM-like polarizations. The realization of two-dimensional photonic crystals with a complete photonic band gap in both polarizations presents therefore a considerable interest. Besides the coupling between TE-like and TM-like polarizations, we note that many materials or internal emitters emit in both polarizations [9, 10]. Thus, a photonic band gap efficient in only one polarization presents a limitation for light coupling to localized optical modes and light extraction from the slab.

In order to solve the limitations associated with light control restricted to only one polarization, Cassagne *et al.* [11] have proposed in 1996 to use new symmetries for photonic crystals. Although not taking into account the vertical confinement of light, their work showed that a lower C_{3v} symmetry applied to the honey-comb lattice leads to the opening of new photonic band gaps.

Another way to reduce the symmetries is to tilt patterns in each elementary cell of a traditional lattice [12, 13]. In the latter studies, the vertical confinement of light was also not taken

into account. To our knowledge, only two studies have taken into account the vertical confinement of light, but the lifting of degeneracy was not sufficiently large to efficiently open photonic band gaps between the first and the second band in both polarizations. A complete photonic band gap of 8.8 % ($\frac{\Delta\omega}{\omega}$) was reported by Bostan *et al.* [14] but only between higher order bands.

Recently, Takayama *et al.* [15] have proposed a modification of traditional photonic crystals by splitting the symmetries of the elementary cell and lifting the degeneracy of optical modes. For this purpose, they proposed to replace in a triangular lattice patterns of C_∞ symmetry with patterns of C_{3v} symmetry and they found a complete photonic band gap in both TE-like and TM-like polarizations. Nevertheless, only a 3.5 % ($\frac{\Delta\omega}{\omega}$) photonic band gap was achieved. Such reduced photonic band gap width is too weak to be used in devices.

In this letter, we investigate the realization of large complete photonic band gaps for both TE-like and TM-like polarizations in symmetric photonic crystal slabs. We concentrate on the achievement of complete photonic band gaps localized between the first and the second band in both polarizations. The investigated slab structures are single mode and the complete band gaps are obtained over the whole Brillouin zone, i.e. are not restricted to the modes below the light cone. This work represents a first step towards the achievement of large complete photonic band gaps in asymmetric photonic crystal slabs like those obtained with silicon-on-insulator substrates. We present two designs of photonic crystals based on C_{3v} symmetries: the first design corresponds to the implementation of the ideas of Cassagne *et al.* to the case of silicon membranes perforated following a honey-comb lattice with different hole sizes; the second design corresponds to a "tri-ellipse" pattern in triangular photonic crystals. Both designs lead to complete photonic band gaps between first and second bands with a width larger than 10 %.

This article is organized as follows: section 2 deals with the C_{6v} and C_{3v} symmetries of photonic crystals. Section 3 presents the results obtained with honey-comb lattices constituted with two different hole sizes, and section 4 presents the results obtained with a "tri-ellipse" triangular lattice.

2.   Photonic crystals with C_{6v} and C_{3v} symmetries

Usually, two-dimensional photonic crystals are constituted with triangular lattices or honey-comb lattices by using constant circular hole sizes. Photonic band diagrams of two-dimensional triangular and honey-comb lattices constituted of air holes drilled in a silicon slab are presented in Fig. 1. In the following calculations, we have used effective indexes of 2.91 and 2.52 for TE-like and TM-like polarizations respectively, which correspond to the effective indexes for a $320\,nm$ thick silicon slab at $1.55\,\mu m$ wavelength. Figure 1(a) shows the example of the triangular lattice with circular holes, where a large band gap is obtained for TE-like polarization, but where no band gap is obtained for TM-like polarization between the first and second band even at very high filling factor. On the contrary, as shown in Fig. 1(b), the honey-comb lattice with the same size of circular holes exhibits a band gap for TM-like polarization, but not for TE-like polarization. The photonic band diagrams show that the symmetries of the lattices do not allow to simultaneously open photonic band gaps in both polarizations.

The symmetries of each wave vector k of the reciprocal space and the symmetries of the associated optical modes depend on the symmetries of the photonic crystal. The triangular lattice or honey-comb lattice using the same circular hole sizes possess a C_{6v} symmetry group, and in the reciprocal space, a K point possesses a C_{3v} symmetry group [16](Fig. 2(a-1)).

A C_{3v} symmetry can lead to degenerated optical modes at the K point as shown by the black curve in Fig. 2(b) corresponding to the band structure of the honey-comb lattice. The degeneracy can be lifted by reducing the symmetry of the photonic crystal, in order to reduce
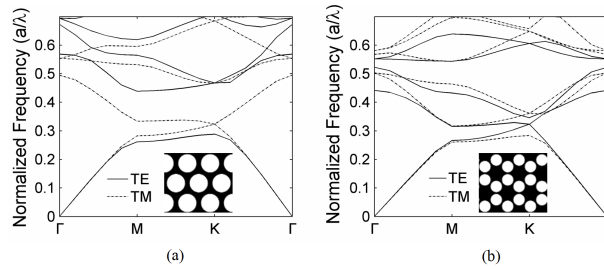
Fig. 1. Photonic band diagrams of photonic crystals of air holes drilled in a high refractive index silicon slab, (a) Triangular photonic crystal with radius $r = 0.4\,a$, (b) Honey-comb lattice with radius $r = 0.25\,a$.

the symmetry of the K point and thus the symmetry of the optical modes. The solutions consist in deleting either the three-fold order rotation symmetry C_3 or the mirror symmetry that can be observed in the representation of the H_z field of the optical modes as shown in Fig. 2(c).

In the case where the C_3 symmetry is deleted, the reduced symmetry increases the anisotropy of the light propagation and contributes to close the band gap. In the case where mirror symmetries are omitted, the light propagation is more isotropic than in the previous case and besides the reduced Brillouin zone is not changed as compared to a lattice with a C_{6v} symmetry (triangular lattice with circular holes) because of time-reversal symmetry properties "$\omega(k) = \omega(-k)$". A C_3 symmetry pattern can be designed in the elementary cells of the triangular lattice, in order to reduce lattice symmetry to C_3 and consequently the K point symmetry. Unfortunately, patterns with only a C_3 symmetry are complicated to design. Another way to decrease the symmetry is to obtain a symmetry mismatch between the real space and the Brillouin zone, i.e. by obtaining mirror symmetry for the patterns which do not correspond to mirror symmetries of the K points. Figure 2(a-2) shows an example where the mirror symmetry $m2$ of the pattern corresponds also to mirror symmetries for the K point. On contrary, Fig. 2(a-3) shows an example of a tilted pattern where the $m1$ mirror symmetry of the pattern is not a mirror symmetry for the K point. The K point symmetry is reduced and it leads to a lifted degeneracy for the optical modes. This effect is illustrated in Fig. 2(b-c-d). In a honey-comb lattice using constant circular hole sizes, the photonic band diagram shown in black in Fig. 2 (b) indicates that the optical modes are degenerate at the K point. A honey-comb lattice with two different hole sizes corresponds to a lattice where the mirror symmetry $m2$ is missing and we can observe in the red band diagram of Fig. 2(b) that the degeneracy is lifted leading consequently to the opening of the band gap. The omission of the mirror symmetry $m2$ can be seen, as expected, on the H_z profile of the modes at K point. In Fig. 2(c), the mirror symmetry m2 exists for the modes of band 1 and band 2 at K point and leads to the existence of even and odd profiles of the electromagnetic field as shown by the imaginary and real parts. In Fig. 2(d), the C_{3v} honey-comb lattice has three mirror symmetries missing and one mirror symmetry is also missing in the mode profile. Note that in the latter case, the H_z component of the optical mode is mostly confined in the small holes or in the large holes. This example shows that the symmetry reduction is an appropriate route to control the degeneracy of band edge optical modes and thus the opening of photonic band gaps. In the following sections, two new designs based on the C_{3v} symmetry are described and studied in details.
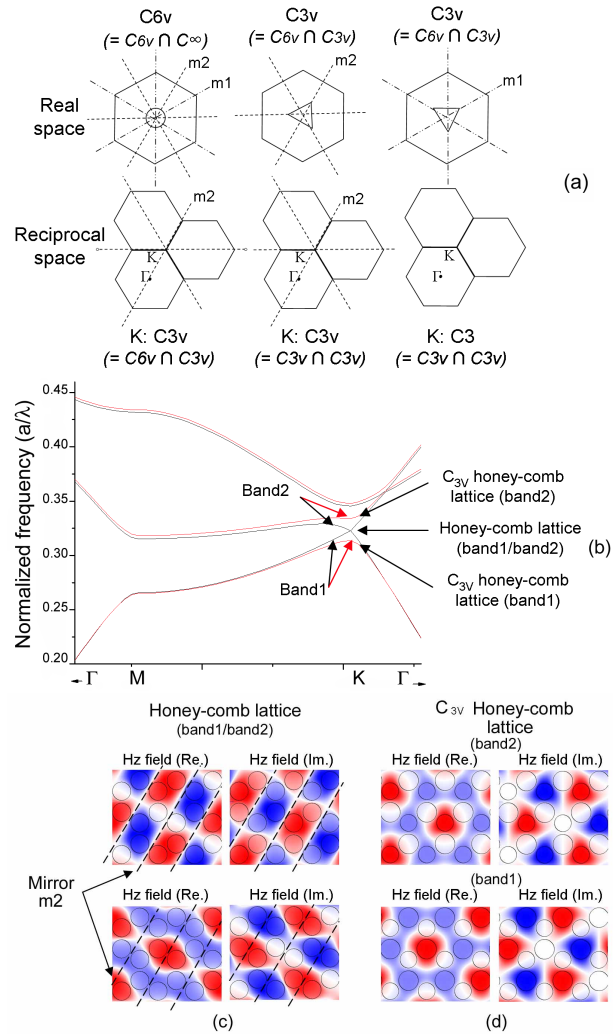
Fig. 2. (a) Drawing of the symmetries in the elementary cells and at the *K* point for a triangular lattice with different patterns: (a-1) Lattice with a C_{6v} symmetry possesses the symmetries associated with *m*1 and *m*2 mirrors, *K* point possesses C_{3v} symmetry with a *m*2 mirror; (a-2) Lattice with a C_{3v} symmetry possesses the *m*2 mirrors, *K* point possesses C_{3v} symmetry with a *m*2 mirror; (a-3) Lattice with a C_{3v} symmetry possesses the *m*1 mirrors, *K* point possesses C_3 symmetry only without *m*1 mirror symmetry. (b) Photonic band diagrams: in black curve, honey-comb lattice with a radius $r = 0.25\,a$ band 1 and band 2 are degenerate at *K* point; in red curve, honey-comb lattice with two radius $r1 = 0.23\,a$ and $r2 = 0.27\,a$, degeneracy at *K* point is lifted. (c) Real and imaginary part of the H_z component of optical modes associated with band 1 and band 2 at the *K* point for honey-comb lattice constituted of similar hole sizes. The *m*2 mirror is shown in the optical mode. Blue and red areas of the optical modes correspond to minimum and maximum magnitudes. (d) Real and imaginary part of the H_z component of optical modes associated with band 1 and band 2 at the *K* point for honey-comb lattice constituted of two different hole sizes. Blue and red areas of the optical modes correspond to minimum and maximum magnitudes.

3. Honey-comb lattices with two different hole sizes

We first discuss the case of a honey-comb lattice which corresponds to a triangular lattice with two holes by elementary cell. The radii of both holes are chosen different to define a C_{3v} symmetry in the photonic crystals, as shown in Fig. 3(a), and to reduce the symmetry of the K point to a C_3 symmetry.

We use the effective index $n(TE) = 2.91$ for TE-like polarization modes and $n(TM) = 2.52$ for TM-like polarization modes. The calculations are performed with the MPB software developed by MIT [5], which is based on a plane-wave expansion method. Parameters for the calculation are the followings: number of bands 10, mesh size 3, and resolution 64.

The band diagram for the first and second bands is shown in Fig. 3(b) according to the reciprocal space path defined. We have investigated the relationship between the band-edge frequency versus the hole sizes. We first present the relationship between the band-edge frequency versus the hole size and secondly the relationship between the band-edge frequency versus the minimum size defined between two neighboring holes.
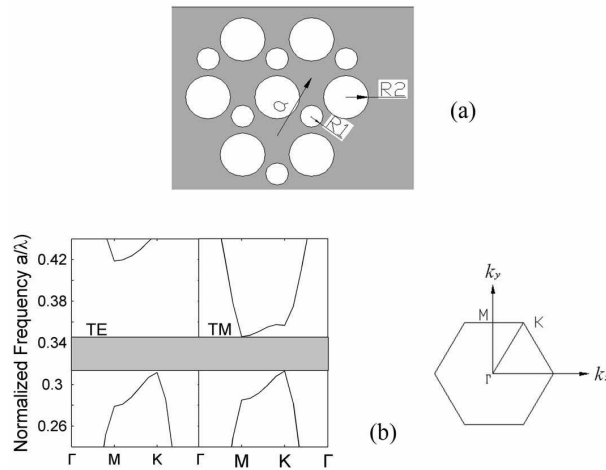

Fig. 3. (a) Honey-comb photonic crystal design with two different hole sizes. (b) Band diagram calculated (according to ΓM and K of the reciprocal space) with optimized photonic band gap for a honey-comb photonic crystal with two different holes sizes ($R1/a = 0.14$, ($R2/a = 0.38$, $n(TE) = 2.91$ and $n(TM) = 2.52$), and drawing of the ΓM and K points in the first Brillouin zone.

In Fig. 4, the R_2 radius is varied whereas the R_1 radius is kept constant and equal to $0.14a$. As the radius R_2 increases, the gap size of TM-like and TE-like polarizations increases, but meanwhile the overlap between the photonic band gaps in TM-like and TE-like polarizations decreases at large hole radii. There is thus an optimum which is obtained for $R_2 = 0.38a$.

We have taken into account an important factor ΔD_{min} which is the minimum distance between two neighboring holes. In practice, it is known that the size of the hole can be very difficult to control accurately in the fabrication process especially when using two different hole sizes because of the proximity effects in lithography process. In addition, the fabrication process can become highly critical if ΔD_{min} is too small. We have thus investigated the dependence of the band-edge frequency on the change of the hole sizes. Figure 5 shows the frequency versus ΔD_{min} which is defined by changing the scale factor β of the two holes ($R_1 = 0.14\beta$, $R_2 = 0.38\beta$) simultaneously. In Fig. 5, the horizontal axis is defined simultaneously by ΔD_{min} and by the scale factor β indicated in square brackets. The β parameter varies between 0.85 and

1.05. As before, we observe that the gap size of TM-like and TE-like polarizations increases, but meanwhile the overlap between the photonic band gaps in TM-like and TE-like polarizations decreases at large hole radius. Optimum sizes of the pattern are obtained for ΔD_{min} equal to $29\,nm$ which corresponds to a β value of 1.
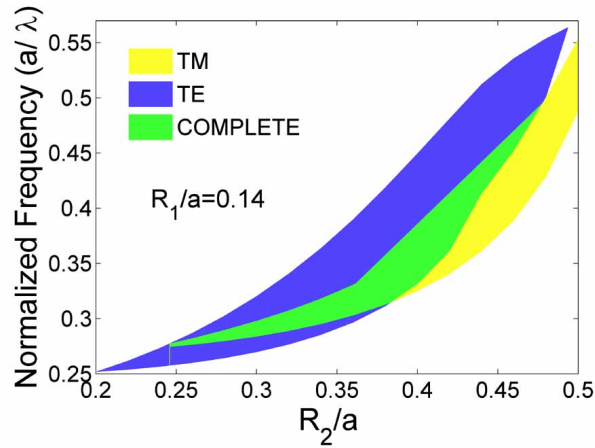

Fig. 4. Gap map in both polarizations for a honey-comb photonic crystal with two different hole sizes versus R_2/a ($R1/a = 0.14$). The blue and yellow areas show the opening of TE and TM photonic band gap and the green one shows the complete photonic band gap.
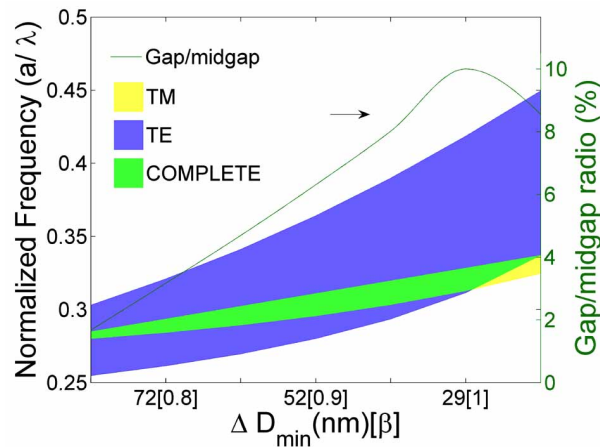

Fig. 5. Gap map in both polarizations for a honey-comb photonic crystal with two different hole sizes versus ΔD_{min}, minimum distance between two holes. The blue and yellow areas show the opening of TE and TM photonic band gaps and the green one shows the complete photonic band gap.

Figures 4 and 5 show first that a maximum gap/midgap ratio ($\frac{\Delta \omega}{\omega}$) of 10 % is obtained for $R_1 = 0.14a$, and $R_2 = 0.38a$, where a is the lattice constant and R_1, R_2 are the radii of the holes respectively. The defined band gap corresponds to a full photonic band gap for both polarizations and the complete band gap lies in the frequency range 0.3128 - 0.3457(c/a). Contrary to Fig. 1, we can see that the TE-like modes are split at the K point. In the same time, the band gap of the TM-like mode is conserved, so a large complete band gap is easily obtained.

We also observe that the gap/midgap ratios ($\frac{\Delta\omega}{\omega}$) are 6.3 %, 8.0 % and 10 % for ΔD_{min} 52 nm, 41 nm and 29 nm respectively. A large complete photonic band gap is obtained even when ΔD_{min} changes in a large range. The optimum reported in Fig. 4 and 5 is thus a robust maximum for which the ΔD_{min} range is compatible with the accuracy of the standard technological processes. Thus, photonic crystals with this design can be realized in a high refractive index contrast slab. The results show that this photonic crystal allow to achieve a photonic band gap larger than the one obtained by Takayama *et al.* ($\frac{\Delta\omega}{\omega} = 3.5$ %) [15] and similar to one obtained by Bostan *et al.* ($\frac{\Delta\omega}{\omega} = 10$ %) [14] between higher order modes.

The effective achievement of a full photonic band gap requires to consider all the guided modes. Andreani *et al.* [17] did recently point out that no complete band gaps appear to be present for the triangular lattice of triangular holes [15] because of the existence of second-order guided modes. In the work of Andreani and coworkers, a free standing high-index slab of thickness d was considered. Their results show that for $d/a = 0.3$, the fundamental TM-like photonic band gap is closed. For $d/a = 0.5$, the band gap for TE-like and TM-like polarizations is open but they do not overlap. For $d/a > 0.5$, the band gap for both polarization modes overlap, but the presence of the higher order mode prevents the opening of complete band gaps. In the same way, Bostan *et al.* did use a slab thickness of $0.6a$ where a is the period of the photonic crystal. This means that for a wavelength $\lambda = 1.55\,\mu m$, the slab thickness is approximately equal to 450 nm. This slab is also not a single-mode waveguide and this feature can reduce and close the gap width which was reported. In addition, in their study, the photonic band gap is only defined below the light cone which is not sufficient if we consider for example emitted light control applications. By taking into account the whole two-dimensional space, the photonic band gap will be diminished since the reported gap is localized between the second and third photonic band. We emphasize that the use of single-mode slab waveguides is particularly important when considering active devices with internal sources. The internal emitters can couple to all the guided modes and a single-mode photonic structure is mandatory to obtain a complete photonic band gap. This requirement might be relaxed when considering photonic structures where external light is coupled with access waveguides. Not all the modes can be excited in the latter case, which can in turn be an advantage to demonstrate experimentally a full band gap.

Here we demonstrate that the honey-comb lattices with two different hole sizes can allow to obtain a complete band gap when d/a is small enough to cut off the second order guided mode. We consider an asymmetric silicon ($\varepsilon = 11.88$) photonic crystal slab of thickness d, with an upper cladding of air and a bottom cladding of buried oxide in which the air hole etching is extended. First the thickness of the silicon slab is chosen in order to be sure that only one fundamental guided mode exists. As the thickness decreases down to 250 nm, the second-order mode is cut off, and the effective index for TE-like modes and TM-like modes are $n(TE) = 2.89$ and $n(TM) = 2.15$ respectively. Considering the midgap frequency for $\lambda = 1.55\,\mu m$, and the following parameters $a = 570nm$ ($d/a = 0.44$), $R_1 = 0.16a$, $R_2 = 0.36a$, the gap width of the complete gap is 8.6%, and the minimum distance between the neighboring holes is 57 nm. We note that even if we decrease the thickness d to 230 nm for a silicon slab membrane configuration, the effective indexes for TE-like and TM-like modes decrease to $n(TE) = 2.83$ and $n(TM) = 1.97$ respectively. For these latter parameters and $a = 645nm$ ($d/a = 0.35$), $R_1 = 0.16a$, $R_2 = 0.36a$, $\Delta D_{min} = 57nm$, a maximum gap/midgap ratio of 6.0 % for the complete band gap is found. As opposed to previous studies, the honey-comb lattice with two different hole sizes shows a large photonic band gap for a single-mode slab and for both polarizations. A ΔD_{min} equal to 57 nm shows that this photonic structure can be realized with standard photonic crystal processing steps.

4. "Tri-ellipse" triangular lattice

The achievement of complete photonic band gaps can also be obtained with new photonic crystal designs without changing the C_{3v} symmetry of the pattern. In this section, we introduce a triangular lattice with a special shape of hole in the elementary cell. The hole is constructed by the overlap of three ellipses which are located at three axes tilted by 120° angle. The "tri-ellipse" shape also presents a C_{3v} symmetry. As shown in Fig. 6(a), the shape of the elementary cell is controlled by three key parameters: the semi-axis lengths A and B, the distance L between the centre of the "tri-ellipse" and the centre of each ellipse. Figure 6(b) shows that the corresponding band structure also presents a complete photonic band gap efficient for both polarizations.
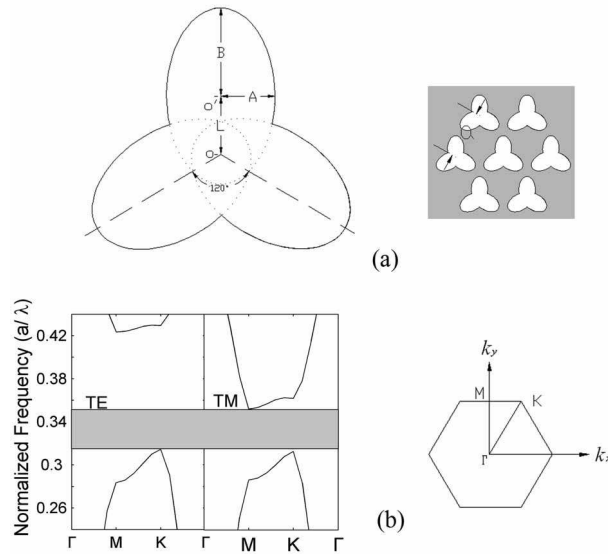

Fig. 6. (a) Triangular photonic crystal design with a "tri-ellipse" shape. (b) Band diagram of the optimized photonic band gap of a triangular photonic crystal with a "tri-ellipse" shape ($L/a = 0.17$, $A/a = 0.27$ and $B/a = 0.3$) and drawing of the Γ M and K points in the first Brillouin zone.

We did also use the effective index $n(TE) = 2.91$ for TE-like polarization modes and $n(TM) = 2.52$ for TM-like polarization modes [15]. The same parameters as before are considered in the calculation. This novel photonic crystal design shows a high similarity in the profile of the different optical modes as compared to the honeycomb lattice with two different hole sizes. To show this similarity, we have plotted in Fig. 7 the H_z and E_z fields of TE-like and TM-like polarizations respectively for both photonic crystals and for both first and second bands.

We have also investigated the relationship between the gap/midgap bandwidth versus the ellipse sizes A and B, and the relationship between the gap/midgap bandwidth as a function of the ellipse position L from the elementary cell center. Figure 8(a) shows the dependence of the gap/midgap ratio versus the semi-axis lengths A and B where each level line shows the gap/midgap value. It reveals that the semi-axis lengths A/a and B/a have a great effect on the band gap width, and that the band gap presents a higher sensitivity according to the semi-axis B (along the three axes) than the semi-axis A. We observe that the overlap between the photonic band gaps in TM-like and TE-like polarizations decreases at large hole sizes (A, B).

These dependencies define optimum sizes for the pattern. Figure 8(b) shows the dependence of gap/midgap versus distance L/a with a maximum for $L = 0.17a$. Reduction of gap/midgap ratio is also observed for high L values.

As shown in Fig. 8, large complete photonic band gaps are also obtained with this pattern. The maximum gap/midgap ratio ($\frac{\Delta\omega}{\omega}$) of 11 % is found for the following parameters $L = 0.17a$, $A = 0.27a$ and $B = 0.3a$, in the frequency range $0.314 - 0.352$ (c/a) as shown in Fig. 6(b). The minimum distance ΔD_{min} between two "tri-ellipse" holes is $55nm$ for the medium wavelength of $\lambda = 1.55\mu m$.
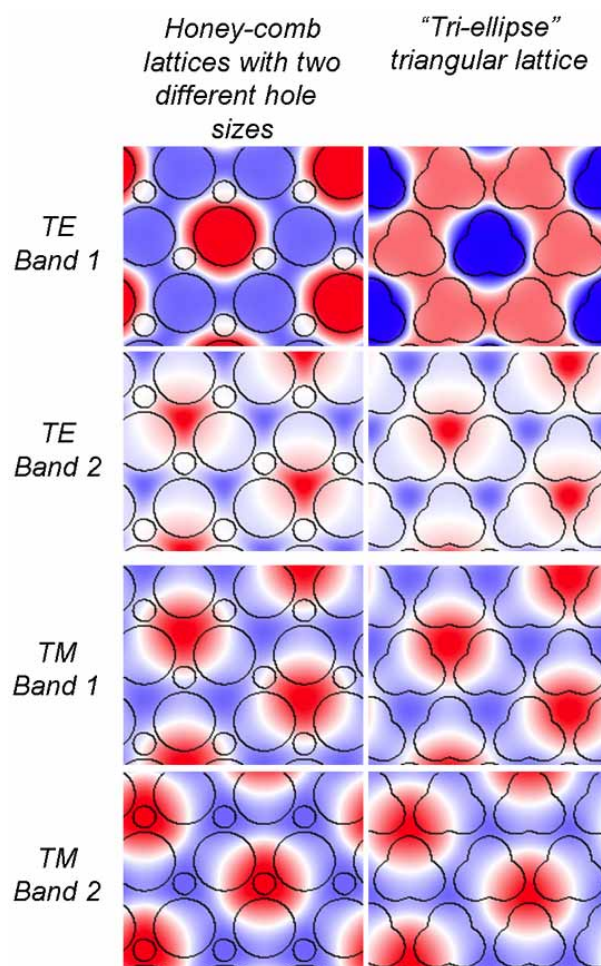

Fig. 7. E_z and H_z fields for TM and TE respectively between honey-comb lattice design with two different hole sizes and "tri-ellipse" triangular lattice. The figure shows both real and imaginary parts of fields and shows the similarity between the mode profiles.

Also, as in the previous section, we have considered Andreani's comments [17] related to the correction of the calculation results for which he did point out that no complete band gaps appear to be present for the triangular lattice of triangular holes due to the large silicon thickness. We did perform the calculation on an asymmetric silicon photonic crystal ($\varepsilon = 11.88$) slab with upper air claddings and bottom silicon dioxide where air holes of the slab are also drilled in the buried oxide. For a thickness of $d = 230nm$, only one mode exists in the slab

membrane and the effective index for both polarizations are $n(TE) = 2.83$ and $n(TM) = 1.97$. With $a = 635\,nm$ ($d/a = 0.36$), a gap/midgap ratio of 8.7 % is found, and the minimum distance between the neighboring holes is $60\,nm$. By slightly changing the shape, the minimum distance between the neighboring holes changes from $21\,nm$ to $97\,nm$ and the gap width changes from 12 % to 5 % respectively.

Similarly to the photonic crystal design discussed in section 3, the "tri-ellipse" shape triangular photonic crystal shows a large complete photonic band gap for a single-mode slab and for both polarizations. These results show that the shape and the size of the hole in the elementary cell have a great effect on opening and overlap of the band gaps. As before, a requirement for ΔD_{min} to be equal to $55\,nm$ also indicates that this photonic crystal can be realized with the standard technological processes.
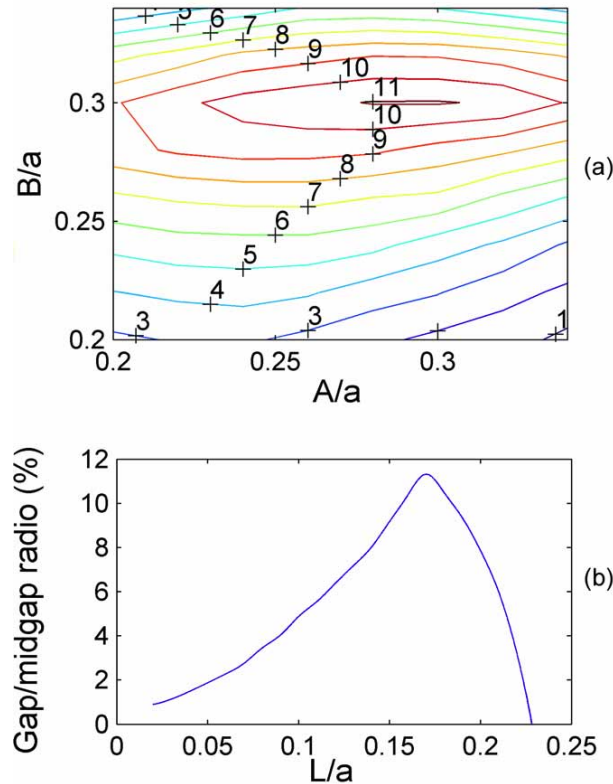

Fig. 8. Gap/midgap map of a triangular photonic crystal with "tri-ellipse" shape. (a) versus semi-axis length A/a and B/a, each colored line defines one percentage of gap/midgap. (b) versus L/a.

We emphasize that the optimization procedure reported in this work is based on two-dimensional calculations. The parameters which maximize the photonic band gap opening might be slightly different when using a 3D calculation of the photonic structure. While beyond the scope of this work, systematic 3D calculations would be necessary to accurately estimate the band gap values and the set of parameters which maximize the band gap opening. However, the same optimization procedure is expected to be effective. Moreover, an additional degree of freedom is available to improve the band gap opening with the three-dimensional control of the lattice pattern, like e.g. an ellipsoidal shape.

Finally, we did concentrate in this work on structures which are expected to be realized with standard technological processes. The lattice designs remain however different from those which are usually used for standard photonic crystals and an optimization of the fabrication process will certainly be required. An important feature is related to the dry etching of the silica. Specific processes which modify the ratio of chemical species in the plasma are now available and should be helpful for the fabrication of photonic structures with complete photonic band gaps.

5. Conclusion

We have performed a detailed numerical study of photonic crystal membranes in high refractive index contrast slabs which exhibit large complete photonic band gaps. This is achieved by reducing the symmetry of the pattern to a C_{3v} symmetry which is properly oriented to reduce the K point symmetry to a C_3 symmetry. The different calculation results show that the honeycomb lattices with two different circular holes or the "tri-ellipse" triangular lattice exhibit strong similarities for light propagation and present a larger overlap of band gaps for both TE-like and TM-like polarizations than the results shown by Takayama *et al.* [15] and Bostan *et al.* [14]. Two main advantages of the proposed designs are: a complete band gap width can be optimized up to 11 % and secondly, the considered structures have a silicon slab thickness of $230\,nm$ as compared to the thickness of $320\,nm$ and more used in the latter works, i.e. the proposed structures are single-mode. We have shown that the hole shapes have a strong impact on the photonic band gap opening and on the overlap of the forbidden bands.